JOURNAL OF CHEMICAL PHYSICS VOLUME 118, NUMBER 19 15 MAY 2003

ARTICLES

Quantum-classical dynamics of nonadiabatic chemical reactions

Alessandro Sergi and Raymond Kapral[a)]
Chemical Physics Theory Group, Department of Chemistry, University of Toronto, Toronto, Ontario M5S 3H6, Canada

(Received 14 January 2003; accepted 19 February 2003)

A reactive flux correlation function formalism for the calculation of rate constants for mixed quantum-classical systems undergoing nonadiabatic dynamics is presented. The linear response formalism accounts for the stationarity of the equilibrium density under quantum-classical dynamics and expresses the rate constant in terms of an ensemble of surface-hopping trajectories. Calculations are carried out on a model two-level system coupled to a nonlinear oscillator which is in turn coupled to a harmonic heat bath. Relevant microscopic species variables for this system include two stable states, corresponding to the ground state adiabatic surface, as well as another species corresponding to the excited state surface. The time-dependent rate constants for the model are evaluated in the adiabatic limit, where the dynamics is confined to the ground Born–Oppenheimer surface, and these results are compared with calculations that account for nonadiabatic transitions among the system states. © *2003 American Institute of Physics.* [DOI: 10.1063/1.1566731]

I. INTRODUCTION

A knowledge of the mechanisms and rates of condensed phase reactive processes is a necessary prerequisite for an understanding of many problems in chemical and biochemical systems. If a condensed phase chemical rate process involves quantum degrees of freedom the calculation of the reaction rate is an especially challenging task. While the earliest derivation of a reactive flux correlation function expression for a rate constant was carried out for a reacting quantum system,[1] the evaluation of such quantum correlation functions remains a difficult task.

The calculation of quantum mechanical rates in many-body environments has been performed using a variety of computational techniques. These include, among others, semiclassical methods,[2] influence-functional techniques,[3] and real-time path integral methods,[4] centroid dynamics,[5] extensions of transition state theory,[6–8] golden rule and Fokker–Planck formulations,[9] and schemes based on mixed quantum-classical surface hopping dynamics.[10–14]

We consider systems where a description in terms of quantum-classical dynamics is appropriate.[15] Situations where the dynamics of the reaction coordinate must be considered to be quantum in nature while all the other degrees of freedom can be described by classical dynamics are not difficult to find. Charge transfer processes involving electronic or protonic degrees of freedom in an environment of heavy atoms are typical examples of systems where quantum-classical dynamics may apply. Since complex and realistic models of the classical environment can be treated by methods based on quantum-classical dynamics, it provides a promising route for the simulation of condensed matter quantum rate processes.

If the classical environment simply provides a slowly varying, almost-static field for the quantum dynamics, a Born–Oppenheimer approximation can be made and adiabatic dynamics can be used to compute the rate. Such calculations are straightforward since the dynamics is purely classical and takes place on a single Born–Oppenheimer surface. In this paper we focus on the calculation of rate constants for systems where such an adiabatic description breaks down.

Our calculations and analysis utilize a formalism that is based on a quantum-classical evolution equation of motion for either the density matrix or dynamical variables.[16–22] Quantum-classical evolution may be expressed in terms of an ensemble of surface-hopping trajectories.[23] By accounting for the distinctive features of quantum-classical dynamics, a formulation of the statistical mechanics of mixed quantum-classical systems and a framework for linear response theory and the calculation of correlation functions has been given.[24,25] These results provide a method for the formulation of correlation function expressions for rate constants in quantum-classical systems and a means to compute them using surface-hopping schemes.

The rate constant formulation we present is general but to illustrate the theory we consider a two-level system coupled to a classical nonlinear oscillator which is in turn coupled to classical harmonic bath. This mimics a physical system where the quantum reactive degree of freedom is directly coupled to a subsystem of the environment and this subsystem is, in turn, coupled to the remaining large number of classical degrees of freedom comprising the rest of the environment. For this model, the identification of the relevant species variables involves both reactant and product states on the ground adiabatic surface as well as the excited adiabatic state. The quantum-classical dynamics accounts for transitions among all of these states. The explicit calculations for this model show how various nonadiabatic transitions contribute to the reaction rate.

[a)] Electronic mail: rkapral@gatto.chem.utoronto.ca

The paper is organized as follows. In Sec. II we derive expressions for the rate constants of a set of coupled reactions using linear response theory. Section III introduces the two-level model we use to illustrate the numerical calculation of nonadiabatic rate constants for quantum-classical systems. In Sec. IV we give a discussion of the phenomenological rate law for the model system that takes into account the existence of an excited state as a third species in the chemical reaction. The linear response results of Sec. II are specialized in Sec. V to derive the explicit form of the time-dependent rate constant for the model. The results of the calculations are presented in Sec. VI along with a discussion of the various contributing terms involving nonadiabatic transitions. Section VII contains the conclusions of this study.

II. RATE CONSTANTS FOR QUANTUM-CLASSICAL SYSTEMS

Consider a quantum system in a classical bath described by the time-independent Hamiltonian operator,

$$\hat{H}_W(R,P)=\frac{P^2}{2M}+\frac{\hat{p}^2}{2m}+\hat{V}_W(\hat{q},R), \tag{1}$$

which is the sum of the classical kinetic energy $P^2/2M$, a quantum kinetic energy operator $\hat{p}^2/2m$, and a potential energy operator $\hat{V}_W(\hat{q},R)$. The subscript W is used to indicate that the quantum-classical description can be derived from a fully quantum one by means of a partial Wigner transform.[22] An intuitive picture of a quantum-classical system is obtained by imagining that for every set of classical phase space coordinates (R,P) one has a Hilbert space upon which the operators $\hat{q}$ and $\hat{p}$ act. Taking this *Eulerian* point of view the dynamics of the classical and quantum degrees of freedom can be consistently formulated and one can derive the quantum-classical Liouville equation for the density matrix $\hat{\rho}_W$ in the form,[22]

$$\frac{\partial\hat{\rho}_W(R,P,t)}{\partial t}=-i\mathcal{L}_W\hat{\rho}_W(t)=-(\hat{H}_W,\hat{\rho}_W(t)). \tag{2}$$

The quantum-classical Liouville operator $i\hat{\mathcal{L}}$ is defined in terms of the algebraic quantum-classical bracket

$$(\hat{H}_W(t),\hat{A}_W)=\frac{i}{\hbar}[\hat{H}_W(t),\hat{A}_W]-\frac{1}{2}(\{\hat{H}_W(t),\hat{A}\}-\{\hat{A},\hat{H}_W(t)\}), \tag{3}$$

where, for any operators $\hat{A}_W$ and $\hat{B}_W$, $[\hat{A}_W,\hat{B}_W]$ is the commutator and $\{\hat{A}_W,\hat{B}_W\}$ is the Poisson bracket. The quantum-classical equilibrium density matrix of the system is stationary under the dynamics and satisfies $(\hat{H}_W,\hat{\rho}_{We})=0$.

The quantum-classical Liouville equation (2) can be derived from the quantum Liouville equation by performing a partial Wigner transform on the bath degrees of freedom, introducing scaled variables $\hat{q}'=\hat{q}/\lambda_m$, $R'=R/\lambda_m$ $\hat{p}'=\hat{p}/p_m$, $P'=P/P_M$, where $\lambda_m=(\hbar^2/m\epsilon_0)^{1/2}$, $p_m=(m\epsilon_0)^{1/2}$, $P_M=(M\epsilon_0)^{1/2}$ with ϵ_0 and $t_0=\hbar/\epsilon_0$ energy and time units, respectively, and finally taking the quantum-classical limit by expanding the propagator to linear order in the small parameter $\mu=(m/M)^{1/2}$.[22] In these scaled variables the quantum-classical bracket and the Liouville operator can be written as

$$(\hat{H}'_W,\hat{A}'_W)=i\mathcal{L}'\hat{A}'_W=i\left[\hat{H}'_W\left(1+\frac{\mu\Lambda'}{2i}\right)\hat{A}'_W-\hat{A}'_W\left(1+\frac{\mu\Lambda'}{2i}\right)\hat{H}'_W\right], \tag{4}$$

where the $\mathcal{O}(\mu)$ dependence is manifest. The operator Λ' is the negative of the Poisson bracket operator in scaled units,

$$\Lambda'=\overleftarrow{\nabla}_{P'}\cdot\overrightarrow{\nabla}_{R'}-\overleftarrow{\nabla}_{R'}\cdot\overrightarrow{\nabla}_{P'}, \tag{5}$$

and the direction of an arrow indicates the direction in which the operator acts.

Suppose we have a multicomponent system where r independent chemical reactions take place. We may associate progress variables, $\overline{\chi_i}$ and affinities $\mathcal{A}_i$ $(i=1,\ldots,r)$, with each independent reaction step. From linear irreversible thermodynamics the chemical rate law describing the time evolution of the reaction rates $\mathcal{J}_i$ takes the following form:[26]

$$\mathcal{J}_i\equiv\frac{d\overline{\chi_i}}{dt}=-\sum_{j=1}^{r}L_{ij}\beta\mathcal{A}_j, \tag{6}$$

Here L_{ij} is an Onsager coefficient.

This rate law can be derived from the microscopic quantum-classical dynamics using linear response theory. In this approach one considers a system subject to external time-dependent forces (affinities) that couple to microscopic progress variables $\hat{\chi}_{Wi}$ so that the hamiltonian is given by

$$\hat{\mathcal{H}}_W(t)=\hat{H}_W-\sum_{i=1}^{r}\hat{\chi}^{\dagger}_{Wi}\mathcal{A}_i(t), \tag{7}$$

where the dagger stands for the adjoint. The dynamical variables are, in general, operators in Hilbert space and functions of the classical phase space variables, $\hat{\chi}_{Wi}(R,P)$.

The chemical rate law can be derived by calculating the nonequilibrium average of $\hat{\chi}_{W,i}$,

$$\mathcal{J}_i\equiv\frac{d\overline{\hat{\chi}_{Wi}(t)}}{dt}=\mathrm{Tr}'\int dR\,dP\,\hat{\chi}_{Wi}\hat{\rho}_W(R,P,t), \tag{8}$$

to linear order in the affinities. Assuming the time dependence of the affinities can be represented by a single Fourier component $\mathcal{A}_i(t)=\exp(i\omega t)\mathcal{A}_i(\omega)$, linear response theory gives

$$\frac{d\overline{\chi_{Wi}}(t)}{dt}=\sum_{j=1}^{r}\Phi_{ij}(\omega)\mathcal{A}_j(t), \tag{9}$$

where the one-sided Fourier transform of the matrix response function is given by

$$\Phi_{ij}(\omega)=\int_0^{\infty}dt\langle(\hat{\chi}_{Wi}(t),\hat{\chi}^{\dagger}_{Wj})\rangle e^{-i\omega t}. \tag{10}$$

While the zero frequency limit of Eq. (9) has the same form as the phenomenological rate law (6), the zero frequency limit of Eq. (10) may be shown to be identically zero. This is the well-known plateau value problem, which is solved by using a projection operator formalism to project out the time variations that occur on the time scale of the chemical relaxation processes. Provided the time scales of the chemical relaxation processes, τ_c, are much slower than those for other microscopic relaxation processes in the system, τ_m, the phenomenological coefficients may be obtained through the correlation function expression,

$$\beta L_{ij} = -\int_0^{t^*} dt'\, Tr' \int dR\, dP\, \hat{\chi}_{Wi}(t')(\hat{\chi}_{Wj}^{\dagger}, \hat{\rho}_{We}), \quad (11)$$

where $\tau_m \ll t^* \ll \tau_c$. In writing this expression we have moved the quantum-classical bracket to act on the equilibrium density and the initial value of the species operator. It is also convenient to define the time-dependent Onsager coefficients by

$$\beta L_{ij}(t) = -\int_0^{t} dt'\, Tr' \int dR\, dP\, \hat{\chi}_{Wi}(t')(\hat{\chi}_{Wj}^{\dagger}, \hat{\rho}_{We}) =$$
$$-Tr' \int dR\, dP\, \hat{\chi}_{Wi}(t)(\hat{\chi}_{Wj}^{\dagger}, \hat{\rho}_{We}), \quad (12)$$

where the time integral has been performed to obtain the second line of Eq. (12). The true phenomenological coefficients, appearing in Eq. (6), may be determined from the plateau value of this expression, should such a plateau exist.

To investigate the validity of the Onsager reciprocal relations among the phenomenological coefficients $L_{ij}(t)$ in quantum-classical dynamics, it is convenient to return to scaled variables in order to explicitly see the dependence on the small parameter μ. Introducing the scaled Onsager coefficient $L'_{ij}(t') = (\hbar/\epsilon_0) L_{ij}(t)$ and the scaled inverse temperature $\beta' = \epsilon_0 \beta$ we can write

$$L'_{ij}(t') = -\frac{1}{\beta'} Tr' \int dR'\, dP'\, \hat{\chi}'_{Wi} e^{-i\hat{\mathcal{L}}' t'} (\hat{\chi}'^{\dagger}_{Wj}, \hat{\rho}'_{We}). \quad (13)$$

Applying the propagator to the bracket yields,[24]

$$e^{-i\hat{\mathcal{L}}' t'} (\hat{\chi}'^{\dagger}_{Wj}, \hat{\rho}'_{We}) = (\hat{\chi}'^{\dagger}_{Wj}(-t'), \hat{\rho}'_{We}) + \mathcal{O}(\mu^2), \quad (14)$$

where we have used the fact that $\hat{\rho}'_{We}$ is stationary under quantum-classical dynamics. Using this result in Eq. (13) we find

$$\begin{aligned} L'_{ij}(t) &= -\frac{1}{\beta'} Tr' \int dR'\, dP'\, \hat{\chi}'^{\dagger}_{Wj}(-t')(\hat{\chi}'_{Wi}, \hat{\rho}'_{We}) + \mathcal{O}(\mu^2) \\ &= -\frac{1}{\beta'} \Big[Tr' \int dR'\, dP'\, \hat{\chi}'_{Wj}(-t') \\ &\quad \times (\hat{\chi}'^{\dagger}_{Wi}, \hat{\rho}'_{We}) \Big]^* + \mathcal{O}(\mu^2) \\ &= \frac{1}{\beta'} \Big[-Tr' \int dR'\, dP'\, \hat{\chi}'_{Wj}(t')(\hat{\chi}'^{\dagger}_{Wi}, \hat{\rho}'_{We}) \Big]^* + \mathcal{O}(\mu^2) \\ &= L'_{ji}(t)^* + \mathcal{O}(\mu^2). \end{aligned} \quad (15)$$

The penultimate line in this equation follows from time reversal symmetry. Equation (15) shows that the Onsager reciprocal relations are valid only to linear order in the small parameter μ in quantum-classical dynamics. In Sec. VI we show that the deviations are negligibly small for our two-level model.

This result has its origin in the action of the quantum-classical propagator on the bracket in Eq. (14) and it is a consequence of the fact that, given three arbitrary operators, within quantum-classical algebra the Jacobi relation holds only to linear order in the small parameter μ:

$$(\hat{A}'_W, (\hat{B}'_W, \hat{C}'_W)) + (\hat{C}'_W, (\hat{A}'_W, \hat{B}'_W)) + (\hat{B}'_W, (\hat{C}'_W, \hat{A}'_W))$$
$$= \mathcal{O}(\mu^2). \quad (16)$$

This discussion establishes the microscopic foundation of the rate law for a reacting quantum-classical system by expressing the Onsager coefficients in terms of equilibrium time correlation functions of the reaction fluxes. In the remaining sections we illustrate the use of this formalism by computing the rate constant for a model system evolving according to nonadiabatic dynamics.

III. TWO-LEVEL SYSTEM COUPLED TO A CLASSICAL BATH

In order to show how the formalism outlined in Sec. II may be used to determine the rate constant, we consider a two-level system coupled to a classical bath. In accord with the standard picture of reaction rates for such systems, the Hamiltonian operator, expressed in a diabatic basis $\{|\uparrow\rangle, |\downarrow\rangle\}$, is taken to have the form

$$\mathbf{H} = \begin{pmatrix} V_n(R_0) + \hbar\gamma_0 R_0 & -\hbar\Omega \\ -\hbar\Omega & V_n(R_0) - \hbar\gamma_0 R_0 \end{pmatrix} + \Bigg(\frac{P_0^2}{2M_0} + \sum_{j=1}^{N} \frac{P_j^2}{2M_j} + \sum_{j=1}^{N} \frac{1}{2} M_j \omega_j^2 R_j^2 - \gamma_b R_0 \sum_{j=1}^{N} c_j R_j \Bigg) \mathbf{I}. \quad (17)$$

This Hamiltonian describes a two-level system directly coupled to a classical nonlinear oscillator with mass M_0 and phase space coordinates (R_0, P_0). The nonlinear oscillator has a quartic potential energy function, $V_n(R_0) = aR_0^4/4 - bR_0^2/2$. The linear coupling to the two-level system is given by $\hbar\gamma_0 R_0 = \hbar\gamma(R_0)$. From the structure of the first 2×2 matrix in Eq. (17) the diabatic energies are given by $E^d_{1,2}(R_0) = V_n(R_0) \pm \hbar\gamma_0 R_0$ and the coupling between the diabatic states is $-\hbar\Omega$. The classical nonlinear oscillator is bilinearly coupled, in turn, to a bath of N independent harmonic oscillators labeled $j = 1, \ldots, N$ with masses M_j and frequencies ω_j. This contribution to the Hamiltonian is described by the second term in Eq. (17), which is proportional to the unit matrix **I**. The coupling strength between the nonlinear oscillator and the harmonic bath is gauged by γ_b and the bilinear coupling is characterized by a spectral density, $J(\omega) = \pi \Sigma_{j=1}^{N} (c_j^2/(2M_j\omega_j^2)) \delta(\omega - \omega_j)$, of Ohmic type where[27,28] $c_j = (\xi\hbar\omega_0 M_j)^{1/2}\omega_j$, $\omega_j = -\omega_c \ln(1 - j\omega_0/\omega_c)$ and $\omega_0 = (\omega_c/N)(1 - e^{-\omega_{\max}/\omega_c})$.

Henceforth, we use a convenient set of dimensionless coordinates $\tilde{R}_0 = (M_0\omega_c/\hbar)^{1/2} R_0$, $\tilde{P}_0 = (\hbar M_0 \omega_c)^{-1/2} P_0$, $\tilde{R}_j = (M_j\omega_c/\hbar)^{1/2} R_j$, and $\tilde{P}_j = (\hbar M_j \omega_c)^{-1/2} P_j$, so that $\tilde{\hat{H}} = \hat{H}/(\hbar\omega_c)$ and the dimensionless parameters of the model are $\tilde{\Omega} = \Omega/\omega_c$, $\tilde{\omega}_j = \omega_j/\omega_c$, $\tilde{c}_j = (\xi\omega_0/\omega_c)^{1/2}\omega'_j$, $\tilde{a} = (\hbar/(M_0^2\omega_c^3))a$, $\tilde{b} = b/(M_0\omega_c^2)$, $\tilde{\gamma}_0 = (\hbar/M_0\omega_c^3)^{1/2}\gamma_0$, and

$\tilde{\gamma}_b=(\hbar/M_0\omega_c)^{1/2}\gamma_b$. The dimensionless reciprocal temperature and time are $\tilde{\beta}=\hbar\omega_c\beta=\hbar\omega_c/k_BT$ and $\tilde{t}=t\omega_c$, respectively. In the following the tilde will be omitted to avoid cluttering the notation but the use of dimensionless units should be understood. Our calculations were carried out for a bath of $N=50$ harmonic oscillators with the following values for the parameters: $\omega_{\max}=3$, $\xi=1$, $\Omega=0.025$, $\gamma_0=1$, $\gamma_b=2$, $a=3$, $b=-2$, and $\beta=6$.

The adiabatic states are obtained by diagonalization of the two-level system Hamiltonian (17) and are given by

$$|1;R_0\rangle=\frac{1}{\mathcal{N}}[(1+G)|\uparrow\rangle+(1-G)|\downarrow\rangle], \tag{18}$$

$$|2;R_0\rangle=\frac{1}{\mathcal{N}}[-(1-G)|\uparrow\rangle+(1+G)|\downarrow\rangle], \tag{19}$$

where $\mathcal{N}(R_0)=\sqrt{2(1+G^2(R_0))}$ with

$$G(R_0)=\frac{1}{\gamma(R_0)}[-\Omega+\sqrt{\Omega^2+\gamma^2(R_0)}]. \tag{20}$$

In the following we use the notation $(R,P)=(R_0,R_1,\ldots,R_N,P_0,P_1,\ldots,P_N)$ for the point in the $2(N+1)$ dimensional phase space of the model. The corresponding adiabatic energies are

$$E_{1,2}(R)=V_b(R)\mp\sqrt{\Omega^2+\gamma^2(R_0)}, \tag{21}$$

where

$$V_b(R)=V_n(R_0)+\sum_{j=1}^{N}\frac{M_j}{2}\omega_j^2R_j^2-R_0\left(\sum_{j=1}^{N}c_jR_j\right). \tag{22}$$

In order to plot the adiabatic energies as a function of the coordinate R_0 we define an adiabatic free energy $W_{1,2}(R_0)$ by

$$e^{-\beta W_{1,2}(R_0)}=\int\prod_{j=1}^{N}dR_j\,Z_{1,2}^{-1}e^{-\beta E_{1,2}(R)}, \tag{23}$$

where $Z_{1,2}=\int dR\exp(-\beta E_{1,2}(R))$. The harmonic degrees of freedom can be easily integrated out to obtain

$$W_{1,2}(R_0)=\beta^{-1}\ln\mathcal{Q}_{1,2}+\frac{a}{4}R_0^4-\frac{b_R}{2}R_0^2\mp\sqrt{\Omega^2+\gamma_0^2R_0^2}, \tag{24}$$

where $b_R=b+\gamma_b^2\Sigma_{j=1}^{N}c_j^2/\omega_j^2$ and

$$\mathcal{Q}_{1,2}=\int dR_0\left[\frac{a}{4}R_0^4-\frac{b_R}{2}R_0^2\mp\sqrt{\Omega^2+\gamma_0^2R_0^2}\right]. \tag{25}$$

These adiabatic free energy curves are shown in Fig. 1. The ground state free energy profile W_1 and the mean profile W_{12} have double-well forms while the excited state W_2 has a single minimum with an avoided crossing at $R_0=0$. The two ground state minima are located at $R_0^{\mp}=\mp 0.99$ and the barrier separating these minima has height $\Delta=1.2$.

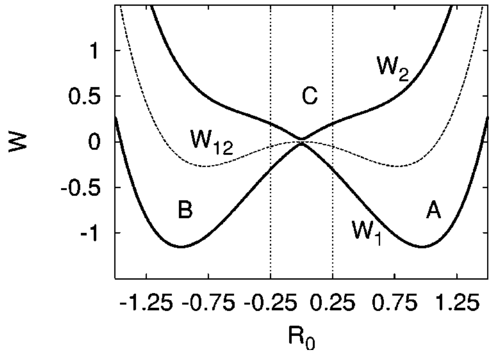

FIG. 1. Free energy surfaces of the model. The bold lines are the ground state and excited state surfaces while the dashed line is the coupled surface. The two vertical dashed lines at $R_0=\pm 0.25$ are the selected window for the calculation (details in the text). The free energy curves defines the three chemical species A, B, and C. A and B, reactant and product, are defined on the ground state surface and they are separated by a vertical line at $R_0=0$ (not drawn in the picture). The species C is defined on the excited state.

IV. PHENOMENOLOGICAL RATE LAWS

The form of a phenomenological rate law depends on the identification of chemical species in the reacting mixture. A guide to the specification of the relevant chemical species for our model system is provided by the structure of the free energy profiles in Fig. 1. The ground state free energy profile has two minima corresponding to two stable states separated by a high barrier at $R_0=0$. Since transitions between these states will occur on a long time scale we are led to identify the positive and negative values of R_0 with species A and B, respectively, when the system is in the ground adiabatic state. Because the system is not restricted to the adiabatic ground state, transitions to the excited single-well adiabatic state may occur and we associate a species C with such configurations. The chemical species defined in this way are indicated schematically in Fig. 1.

We are then led to consider the following chemical reactions among the three species:

$$I\underset{k_{JI}}{\overset{k_{IJ}}{\rightleftharpoons}}J,\quad I<J=A,B,C, \tag{26}$$

where k_{IJ}, $I\neq J=A,B,C$ are the transition probabilities for $I\rightarrow J$. The transition probabilities are normalized so that $\Sigma_{J=A}^{C}k_{IJ}=1$. In such an unimolecular scheme where all possible reactions take place among the components, only two of the three reactions are independent. Following de Groot and Mazur[26] we may formulate the irreversible thermodynamics for this case in terms of two independent species and the corresponding affinities in place of the r independent reactions considered in the general formulation in Sec. II. In this circumstance we may write the entropy production in the form

$$\sigma=-\sum_{I=A}^{B}\frac{d\overline{n_I}}{dt}\beta\mathcal{A}_{IC}(t), \tag{27}$$

where $d\overline{n_I}/dt$ is a reactive flux and $\mathcal{A}_{IC}(t)=\mu_C(t)-\mu_I(t)$ is the corresponding affinity, $(I=A,B)$. The linear phenomenological laws now take the form

$$\frac{d\overline{n_I}}{dt}=-\sum_{J=A}^{B}L_{IJ}\beta\mathcal{A}_{IC}(t), \tag{28}$$

for $I=A,B$. We may compare this phenomenological rate law with that assuming mass action kinetics,

$$\frac{d\overline{n_I}}{dt}=\sum_{J=A}^{B}(k_{JI}-\delta_{JI})\left(\overline{n_J}-\frac{\overline{n_J^{\mathrm{eq}}}}{\overline{n_C^{\mathrm{eq}}}}\overline{n_C}\right), \tag{29}$$

for $I=A,B$. If we write $\mu_I=\mu_I^o+k_BT\ln\overline{n_I}$ as is appropriate for dilute reacting species, and assume small deviations from equilibrium, we may identify the phenomenological coefficients as

$$L_{IJ}=(k_{JI}-\delta_{JI})\overline{n_J^{\mathrm{eq}}}, \tag{30}$$

for $I,J=A,B$. We have the relations $L_{AA}(\overline{n_A^{\mathrm{eq}}})^{-1}=k_{AA}-1=-(k_{AB}+k_{AC})$ which describes the net decay of species A and $L_{BA}(\overline{n_A^{\mathrm{eq}}})^{-1}=k_{AB}$, with similar relations for L_{BB} and L_{AB}. In view of the symmetry of the model there are only two independent rate constants which may be expressed in terms of the two Onsager coefficients L_{AA} and L_{BA}.

V. TIME-DEPENDENT RATE COEFFICIENT

Using the results of Secs. II and IV we may write expressions for the time-dependent Onsager coefficients for our model. The general linear response results given in Sec. II may be specialized to our unimolecular reaction case by writing the time-dependent Hamiltonian as

$$\hat{\mathcal{H}}_W(t)=\hat{H}_W-\sum_{I=A}^{B}\hat{\chi}_{WI}^{\dagger}\mathcal{A}_{IC}(t), \tag{31}$$

where the sum is over the two independent species. The linear response analysis then leads to

$$L_{IJ}(t)=-\frac{1}{\beta}\mathrm{Tr}'\int dR\,dP\,\hat{\chi}_{WI}(t)(\hat{\chi}_{WJ},\hat{\rho}_{We}). \tag{32}$$

Equation (32) provides a microscopic expression for the time-dependent Onsager coefficient in terms of a quantum-classical progress variable $\hat{\chi}_{W,I}(t)$ and the quantum-classical bracket of the progress variable at time zero with the stationary density matrix. To simplify the notation we drop the W subscript on species variables.

In order to evaluate this expression we must choose specific microscopic forms for the species variables. In view of the discussion in Sec. IV, operators for the A, B, and C species may be defined as

$$\begin{aligned}\hat{N}_A&=|1;R_0\rangle\Theta(R_0)\langle 1;R_0|,\\ \hat{N}_B&=|1;R_0\rangle\Theta(-R_0)\langle 1;R_0|,\\ \hat{N}_C&=|2;R_0\rangle\langle 2;R_0|,\end{aligned} \tag{33}$$

where $\Theta(\pm R_0)$ is the Heaviside function selecting the right or left wells and $|I;R_0\rangle\langle I;R_0|$ is a projector onto the adiabatic state $|I;R_0\rangle$. Note that $\Sigma_{I=A}^{C}\hat{N}_I=1$, consistent with the fact that the combined Hilbert and configuration space is completely partitioned into regions corresponding to the three species.

Consider the calculation of $L_{BA}(\overline{n_A^{\mathrm{eq}}})^{-1}=k_{AB}$. Using Eq. (32) and the definition (30) we have

$$\begin{aligned}k_{AB}(t)&=-(\beta\overline{n_A^{\mathrm{eq}}})^{-1}\mathrm{Tr}'\int dR\,dP\,\hat{\chi}_B(t)(\hat{\chi}_A,\hat{\rho}_{We}),\\ &=-(\beta\overline{n_A^{\mathrm{eq}}})^{-1}\sum_{\alpha\alpha'}\int dR\,dP\,\chi_B^{\alpha'\alpha}(t)(\hat{\chi}_A,\hat{\rho}_{We})_{\alpha\alpha'}.\end{aligned} \tag{34}$$

The second line of Eq. (34) introduces the adiabatic basis to compute the trace. Given the fact that $\hat{\chi}_A(t)=-\hat{\chi}_B(t)-\hat{\chi}_C(t)$ in view of total number conservation, we may substitute this expression into Eq. (32) for $L_{AA}(t)$ and use Eq. (34) to deduce that

$$k_{AC}(t)=-(\beta n_A^{\mathrm{eq}})^{-1}\mathrm{Tr}'\int dR\,dP\,\hat{\chi}_C(t)(\hat{\chi}_A,\hat{\rho}_{We}). \tag{35}$$

These correlation function expressions can be used to compute k_{AB} and k_{AC}, thus determining the two independent rate constants in the problem.

Representation of the species variables in the adiabatic basis gives $\hat{N}_A^{\alpha\alpha'}=\delta_{\alpha1}\delta_{\alpha'1}\Theta(R_0)$, $\hat{N}_B^{\alpha\alpha'}=\delta_{\alpha1}\delta_{\alpha'1}\Theta(-R_0)$ and $\hat{N}_C^{\alpha\alpha'}=\delta_{\alpha2}\delta_{\alpha'2}$. The progress variable $\hat{\chi}_A$, which is defined as the deviation of $\hat{N}_A$ from its equilibrium value, may be replaced by $\hat{N}_A$ when computing Eq. (34). We use the dimensionless variables introduced Sec. III and express the time-dependent rate coefficients in units of ω_c.

The mixed quantum-classical bracket in Eq. (34) takes the following form in the adiabatic basis:

$$\begin{aligned}(\hat{N}_A,\hat{\rho}_{We})_{\alpha\alpha'}=&\,i\Theta(R_0)(\delta_{\alpha1}-\delta_{\alpha'1})\rho_{We}^{\alpha\alpha'}\\ &-\frac{1}{2}\frac{\partial\Theta(R_0)}{\partial R_0}(\delta_{\alpha1}+\delta_{\alpha'1})\frac{\partial\rho_{We}^{\alpha\alpha'}}{\partial P_0}\\ &-\frac{1}{2}\Theta(R_0)\Bigg(d_{\alpha1}\frac{\partial\rho_{We}^{1\alpha'}}{\partial P_0}-\frac{\partial\rho_{We}^{\alpha1}}{\partial P_0}d_{1\alpha'}\\ &-\delta_{\alpha1}\sum_{\beta}d_{1\beta}\frac{\partial\rho_{We}^{\beta\alpha'}}{\partial P_0}\\ &+\sum_{\beta}\frac{\partial\rho_{We}^{\alpha\beta}}{\partial P_0}d_{\beta1}\delta_{\alpha'1}\Bigg),\end{aligned} \tag{36}$$

where the nonadiabatic coupling matrix element is

$$d_{\alpha\alpha'}=\langle\alpha;R_0|\partial/\partial R_0|\alpha';R_0\rangle, \tag{37}$$

and we have used the fact that

$$\left\langle\alpha;R_0\left|\frac{\partial\hat{N}_A}{\partial R_0}\right|\alpha';R_0\right\rangle=\frac{\partial N_A^{\alpha\alpha'}}{\partial R_0}+\sum_{\gamma=1}^{2}(d_{\alpha\gamma}N_A^{\gamma\alpha'}-N_A^{\alpha\gamma}d_{\gamma\alpha'}). \tag{38}$$

In the following we will also assume the adiabatic basis to be real so that $d_{11}=d_{22}=0$ and $d_{12}=-d_{21}$. The equilibrium density matrix $\rho_{We}^{\alpha\alpha'}$ is stationary under quantum-classical evolution but its explicit form is not known in general. However, it is known to order $\hbar$ and to this order it coincides with the exact quantum canonical density matrix. To this first order in $\hbar$ (in dimensionless units) it is given by[24]

$$\rho_{We}^{\alpha\alpha'} \approx \rho_{We}^{(0)\alpha}\delta_{\alpha\alpha'} - i f_{We}^{\alpha\alpha'}(1-\delta_{\alpha\alpha'}), \tag{39}$$

where

$$\rho_{We}^{(0)\alpha} = Z_0^{-1} e^{-\beta H_W^\alpha}, \quad Z_0 = \sum_\alpha \int dR\, dP\, e^{-\beta H_W^\alpha}, \tag{40}$$

and

$$f_{We}^{\alpha\alpha'} = P_0 \cdot d_{\alpha\alpha'} \rho_{We}^{(0)\alpha}\left(\frac{\beta}{2}(1+e^{-\beta E_{\alpha'\alpha}}) + \frac{1-e^{-\beta E_{\alpha'\alpha}}}{E_{\alpha\alpha'}}\right), \tag{41}$$

with $\alpha,\alpha'=1,2$. Equation (39) gives also the decomposition of the density matrix into diagonal and off-diagonal parts. From Eq. (41) it is clear that $\rho_{We}^{12}=(\rho_{We}^{21})^*$ and $\rho_{We}^{12}+\rho_{We}^{21}=0$. The diagonal and off-diagonal contributions to the density matrix can be substituted into Eq. (36) and the time-dependent rate coefficient in Eq. (34) can be decomposed into the sum of three contributions:

$$k_{AB}(t) = k_{AB}^{d}(t) + k_{AB}^{o1}(t) + k_{AB}^{o2}(t). \tag{42}$$

The diagonal part of the density matrix gives rise to the contribution

$$k_{AB}^{d}(t) = (\beta n_A^{\mathrm{eq}})^{-1} \int dR\, dP\, N_B^{11}(R,P,t) \frac{\partial \Theta(R_0)}{\partial R_0} \frac{\partial \rho_{We}^{11}}{\partial P_0}, \tag{43}$$

while the off-diagonal part of the density matrix yields the following two terms

$$k_{AB}^{o1}(t) = (\beta n_A^{\mathrm{eq}})^{-1} \int dR\, dP\, \mathrm{Im}\{N_B^{12}(R,P,t)\} \times \frac{\partial \Theta(R_0)}{\partial R_0} \frac{\partial f_{We}^{12}}{\partial P_0}, \tag{44}$$

$$k_{AB}^{o2}(t) = -2(\beta n_A^{\mathrm{eq}})^{-1} \int dR\, dP\, \mathrm{Re}\{N_B^{12}(R,P,t)\}\Theta(R_0) \times \beta d_{12} P_0 \rho_{We}^{11} \frac{1-e^{-\beta E_{21}}}{\beta E_{12}}. \tag{45}$$

Equations (43)–(45) provide well-defined formulas to calculate the time-dependent rate coefficient $k_{AB}(t)$ from whose plateau value the rate constant k_{AB} may be determined.

A completely analogous set of formulas can be used to compute k_{AC} by replacing $N_B^{\alpha\alpha'}(t)$ by $N_C^{\alpha\alpha'}(t)$ in Eq. (44) and (45).

VI. CALCULATION AND RESULTS

A numerical scheme to compute the time-dependent rate coefficient given by Eqs. (43)–(45) requires a sampling procedure to evaluate the ensemble averages over the classical and quantum degrees of freedom, and a method to compute the time evolution of dynamical variables $\chi_I^{\alpha\alpha'}(R,P,t)$ under quantum-classical dynamics.

In general the initial classical phase space coordinates (R,P) can be sampled, using the diagonal part of the stationary density matrix as a weight function, by means of a variety of molecular dynamics or Monte Carlo techniques. In the case of our model (R,P) can be directly sampled from ρ_{We}^{11} using Gaussian random numbers with the proper mean deviation. For the phase space sampling in Eqs. (43) and (44), R_0 is fixed at the barrier top. The evaluation of Eq. (45) requires an analogous scheme apart from the fact that R_0 is uniformly sampled in the reactant (species A) well.

To compute the quantum-classical evolution of $\chi_I^{\alpha\alpha'}(R,P,t)$ we must solve the equation of motion,

$$\frac{d\chi_I^{\alpha\alpha'}(R,P,t)}{dt} = \sum_{\nu\nu'} i\mathcal{L}_{\alpha\alpha',\nu\nu'} \chi_I^{\nu\nu'}(R,P,t), \tag{46}$$

where the evolution operator in the adiabatic basis is given by[22]

$$\begin{aligned} i\mathcal{L}_{\alpha\alpha',\nu\nu'} &= i\mathcal{L}^{(0)}_{\alpha\alpha'}\delta_{\alpha\nu}\delta_{\alpha'\nu'} - J_{\alpha\alpha',\nu\nu'} \\ &= (i\omega_{\alpha\alpha'} + iL_{\alpha\alpha'})\delta_{\alpha\nu}\delta_{\alpha'\nu'} - J_{\alpha\alpha',\nu\nu'}. \end{aligned} \tag{47}$$

Here $\omega_{\alpha\alpha'} = (E_\alpha - E_{\alpha'})/\hbar \equiv E_{\alpha\alpha'}/\hbar$ and

$$iL_{\alpha\alpha'} = \frac{P}{M}\cdot\frac{\partial}{\partial R} + \frac{1}{2}(F_W^\alpha + F_W^{\alpha'})\cdot\frac{\partial}{\partial P}, \tag{48}$$

where

$$F_W^\alpha = -\left\langle \alpha;R \left| \frac{\partial \hat{V}_W(\hat{q},R)}{\partial R} \right| \alpha;R \right\rangle$$

is the Hellmann–Feynman force for state α. The operator J that gives rise to nonadiabatic dynamics is

$$\begin{aligned} J_{\alpha\alpha',\nu\nu'} = &-\frac{P}{M}\cdot d_{\alpha\nu}\left(1+\frac{1}{2}S_{\alpha\nu}\cdot\frac{\partial}{\partial P}\right)\delta_{\alpha'\nu'} \\ &- \frac{P}{M}\cdot d^*_{\alpha'\nu'}\left(1+\frac{1}{2}S^*_{\alpha'\nu'}\cdot\frac{\partial}{\partial P}\right)\delta_{\alpha\nu}. \end{aligned} \tag{49}$$

The quantity $S_{\alpha\nu}$ is defined as

$$S_{\alpha\nu} = E_{\alpha\nu} d_{\alpha\nu}\left(\frac{P}{M}\cdot d_{\alpha\nu}\right)^{-1}. \tag{50}$$

The solution of Eq. (46) in terms of a sequence of surface-hopping trajectories was discussed in earlier papers.[22,23,25] Using the symbol $s_i=(\alpha_i\alpha_i')$ to refer to the pair of quantum state indices, we may write the solution of Eq. (46) as

$$\begin{aligned} \chi_I^{s_0}(R,P,t) = e^{\mathcal{L}^0_{s_0}t}\chi_I^{s_0}(R,P) + \sum_{n=1}^{\infty}(-1)^n \sum_{s_1\ldots s_n}\int_0^t d\tau_1 \\ \times \int_{\tau_1}^t d\tau_2 \cdots \int_{\tau_{n-1}}^t d\tau_n \\ \times \prod_{k=1}^{n}[e^{i\mathcal{L}^0_{s_{k-1}}(\tau_k-\tau_{k-1})} J_{s_{k-1}s_k}] \\ \times e^{i\mathcal{L}^0_{s_n}(t-\tau_n)}\chi_I^{s_n}(R,P). \end{aligned} \tag{51}$$

In Eq. (51) n labels the number of nonadiabatic transitions. To evaluate this expression we use the fact that the action of the diagonal part of the evolution operator on any phase space function is given by

$$\begin{aligned} e^{i\mathcal{L}^0_{s_j}t} f_{s_j}(R,P) &= \exp\left(\int_0^t d\tau\, \omega_{s_j}(\overline{R}_{s_j,\tau})\right) e^{iL_{s_j}t} f_{s_j}(R,P) \\ &\equiv \mathcal{W}_{s_j}(t,0) f_{s_j}(\overline{R}_{s_j,t}, \overline{P}_{s_j,t}). \end{aligned} \tag{52}$$

The forward-evolved classical trajectory segment is defined as the trajectory that starts at (R,P) at time 0 and ends at $(\overline{R}_{s_j,t},\overline{P}_{s_j,t})$ at time t:

$$(\overline{R}_{s_j,t},\overline{P}_{s_j,t})=e^{iL_{s_j}t}(R,P). \tag{53}$$

The constant-energy trajectory segments entering in the quantum-classical evolution have been numerically integrated using a time-reversible algorithm[29] and a time step $dt=0.01$. The phase factor $\mathcal{W}_{s_j}(t,0)$ associated with the classical evolution segment is nontrivial when the evolution occurs on the mean of two adiabatic surfaces and it must be properly taken into account.

The operator J is evaluated in the momentum-jump approximation. Noticing that[25]

$$\begin{aligned}\frac{1}{2}S_{\alpha_j\alpha_k}\cdot\frac{\partial}{\partial P}&=\frac{1}{2}E_{\alpha_j\alpha_k}d_{\alpha_j\alpha_k}\left(\frac{P}{M}\cdot d_{\alpha_j\alpha_k}\right)^{-1}\cdot\frac{\partial}{\partial P}\\&=E_{\alpha_j\alpha_k}M_0\frac{\partial}{\partial(P_0\hat{d}_{\alpha_j\alpha_k})^2},\end{aligned} \tag{54}$$

and approximating $(1+1/2\ S_{\alpha_j\alpha_k}\cdot\nabla_P)\approx\exp(1/2\ S_{\alpha_j\alpha_k}\cdot\nabla_P)$ we may express J as

$$\begin{aligned}J_{\alpha_j\alpha_k,\alpha_j'\alpha_k'}\approx&-\frac{P_0}{M_0}d_{\alpha_j\alpha_k}e^{[E_{\alpha_j\alpha_k}M_0\partial/\partial(P_0\hat{d}_{\alpha_j\alpha_k})^2]}\\&-\frac{P_0}{M_0}d_{\alpha_a'j\alpha_k'}e^{[E_{\alpha_j'\alpha_k'}M_0\partial/\partial(P_0\hat{d}_{\alpha_j'\alpha_k'})^2]}.\end{aligned} \tag{55}$$

The action of the operators in J on any function of the momentum is given by

$$e^{\Delta E_{\alpha_j\alpha_k}M_0\partial/\partial(P\cdot\hat{d}_{\alpha_j\alpha_k})^2}f(P)=f(P+\hat{d}_{\alpha_j\alpha_k}\cdot\Delta P_0), \tag{56}$$

where

$$\begin{aligned}\Delta P_0=&-\hat{d}_{\alpha_j\alpha_k}(\hat{d}_{\alpha_j\alpha_k}\cdot P_0)+\hat{d}_{\alpha_j\alpha_k}\,\mathrm{sgn}(P_0\cdot\hat{d}_{\alpha_j\alpha_k})\\&\times\sqrt{(P_0\cdot\hat{d}_{\alpha_j\alpha_k})^2+E_{\alpha_j\alpha_k}M_0}.\end{aligned} \tag{57}$$

All the other components are identically zero because in our model only the coordinate R_0 is coupled to the quantum subsystem.

For a fixed time interval t and a fixed number of jumps Eq. (51) provides a well defined algorithm for the computation of the time evolution of the species variables. One can sample the times, τ_i, $i=1,\ldots,n$, when the quantum jumps occur from a uniform distribution. One has also to sample, with probability 1/2, which of the two terms in Eq. (49) acts.

A. Adiabatic dynamics

In the adiabatic limit the dynamics is restricted to the ground adiabatic state. Only the first term in Eq. (51) contributes and the time-dependent rate coefficient in Eqs. (42) and (43) reduces to

$$k_{AB}^{\mathrm{ad}}(t)=\frac{1}{\overline{n_A^{\mathrm{eq}}}}\int dR\,dP(e^{iL_{11}t}\Theta(R_0))\,\delta(R_0)\,\frac{P_0}{M_0}\rho_{We}^{11}. \tag{58}$$

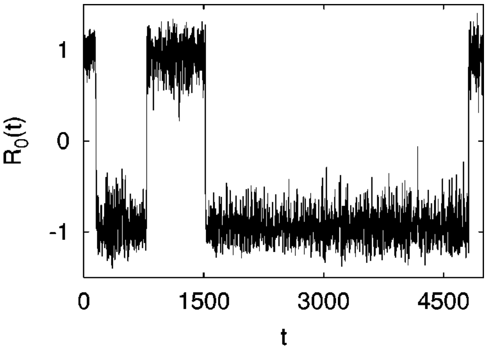

FIG. 2. Time series of the coordinate $R_0(t)$ along a trajectory evolving on the ground state surface, typical of classical activated barrier crossing dynamics.

This is the standard reactive flux autocorrelation expression for a classical activated barrier crossing problem. The time evolution of $R_0(t)$ under this ground state adiabatic dynamics is shown in Fig. 2. One can see the infrequent transitions between the two stable states of the bistable potential characteristic of an activated process.

The $t=0+$ value of $k_{AB}^{\mathrm{ad}}(t)$ gives the transition state theory approximation to the rate constant,[30]

$$\begin{aligned}k_{AB}^{\mathrm{TST}}=k_{AB}^{\mathrm{ad}}(t=0+)&=n_{A,\mathrm{eq}}^{-1}\langle\Theta(P_0)P_0\delta(R_0)\rangle,\\&=\sqrt{\frac{2}{\beta\pi}}\frac{e^{\beta\Omega}}{\mathcal{Q}}.\end{aligned} \tag{59}$$

For the parameters of our model we find $k_{AB}^{\mathrm{TST}}=4.5\times10^{-4}$. The time-dependent transmission coefficient is defined as the ratio $k_{AB}^{\mathrm{ad}}(t)/k_{AB}^{\mathrm{TST}}$ and this quantity is plotted in Fig. 3. One can identify a ''plateau'' which starts at approximately $t=3$, after which the transmission coefficient decays slowly to zero on the chemical relaxation time scale. Consequently, for the chosen parameter values, the model exhibits a well-defined rate process in the adiabatic limit.

B. Nonadiabatic dynamics

Before presenting the results for the rate constants using nonadiabatic dynamics, we give some additional details of the simulation scheme used in their evaluation.

An important feature of quantum-classical dynamics is that oscillatory quantum phase factors $\mathcal{W}_{\alpha\alpha'}(t)$ are linked to

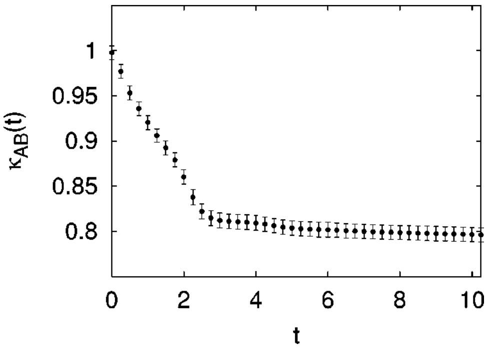

FIG. 3. Transmission coefficient $\kappa_{AB}(t)=k_{AB}^{\mathrm{ad}}(t)/k_{AB}^{\mathrm{TST}}$ vs time for adiabatic dynamics.

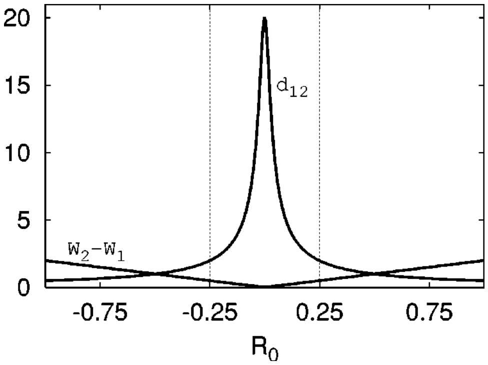

FIG. 4. Nonadiabatic coupling matrix element (labeled d_{12}) and adiabatic free energy difference $W_2(R_0)-W_1(R_0)$ vs R_0. The window discussed in the text is indicated by two vertical lines at $R_0=\pm 0.25$.

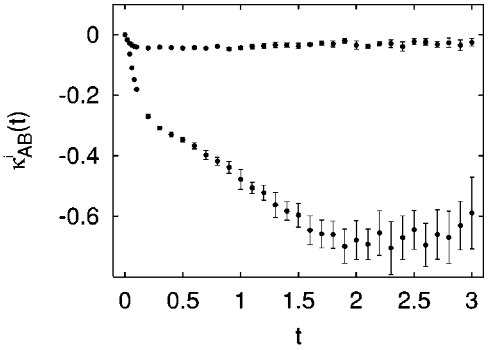

FIG. 5. Time-dependent rate coefficients $\kappa_{AB}^{d}(t)=k_{AB}^{d}(t)/k_{AB}^{\mathrm{TST}}$ (lower curve) and $\kappa_{AB}^{o2}(t)=k_{AB}^{o2}(t)/k_{AB}^{\mathrm{TST}}$ (upper curve) vs time showing the diagonal two-jump and off-diagonal one-jump contributions, respectively.

classical trajectory segments on the mean surfaces. For long times and large energy gaps these phase factors rapidly oscillate. The rapidly oscillating phases are canceled by destructive interference with other trajectories in the ensemble with nearby initial conditions, consistent with the fact that the system should lie on the adiabatic surfaces outside the region of strong interaction.

The algorithm for the evaluation of the quantum-classical propagation in Eq. (51) forces the nonadiabatic transitions to occur at the sampled times τ_i, $i=1,\ldots,n$, regardless of the value of energy gap and nonadiabatic coupling matrix element $d_{\alpha\alpha'}$, at phase points evaluated at times τ_i. The nonadiabatic coupling matrix element $d_{\alpha\alpha'}$ in Eq. (37) acts as a statistical weight for every nonadiabatic transition. The physics of the problem suggests a way to circumvent this difficulty. The probability of jumping between the adiabatic surfaces is high in a narrow region of R_0 around the barrier top where the energy gap is small and $d_{\alpha\alpha'}$ is large (see Fig. 4).

One can reasonably expect that once the coordinate $R_0(t)$ lies outside this small region, the probability of a nonadiabatic transition will be small, as an inspection of the nonadiabatic coupling matrix as a function of R_0 shows. Thus, in our calculations, we have used a window for the R_0 coordinate, $-0.25\leqslant R_0\leqslant 0.25$, around the barrier top $R_0=0$ (see Figs. 1 and 4) within which nonadiabatic transitions occur. A nonadiabatic contribution was counted with a unit weight only if $R_0(t)$ at the moment of the transition was inside this window, otherwise it was given a zero weight. We have confirmed that the results are insensitive to the precise value of the size of the window provided it covers the important region around the barrier top. We tested the approximation using a larger window of $-0.5\leqslant R_0\leqslant 0.5$ and no appreciable difference in the results was observed, apart from an increase of the statistical error consistent with the interpretation of the effect of the above-given phase factors. This approximation should be contrasted with schemes that force the transition to occur strictly and only at the barrier top.[14]

The action of the momentum-jump operator in Eq. (55) on a function $f(P_0)$ can be approximated by $f(P_0+\hat{d}_{\alpha_j\alpha_k}\cdot\Delta P_0)$. If there is insufficient kinetic energy corresponding to the bath momentum along $\hat{d}_{\alpha_j\alpha_k}$, ΔP_0 defined in Eq. (57) will be imaginary. In this case no transition was permitted to occur and the contribution of the trajectory to the rate constant was set to zero. Occasionally ΔP_0 can take large values where the momentum-jump approximation fails. For this reason quantum jumps with high momentum shifts $\Delta P_0>\hat{d}_{\alpha_j\alpha_k}\cdot\Delta P_0^c$ were removed from the ensemble. In our calculation we have used $\Delta P_0^c=2$.

While the results presented in the following can be obtained using relatively few trajectories for short times ($t<2$) we used 4×10^6 trajectories for longer times to reduce the statistical errors. Statistical fluctuations are larger for these times because of the incomplete cancellation of the phase factors in the ensemble. In addition we have constructed the algorithm to be able to examine the contributions to the rate from fixed numbers of nonadiabatic transitions which places additional demands on the computation. Other more efficient schemes can be used to compute the rate constant directly without computing these individual contributions.[31–33]

The evaluation of the rate constant for nonadiabatic dynamics entails the computation of the three terms in Eq. (42) which describe different contributing factors to the reaction rate. The "diagonal" term $k_{AB}^{d}(t)$ in Eq. (43) has nonadiabatic contributions arising from even numbers of quantum transitions. The contribution with no nonadiabatic transitions is just the adiabatic result discussed earlier. The two-jump contribution, normalized by k_{AB}^{TST}, is shown in Fig. 5. This contribution starts at zero for $t=0$ and quickly decays to a plateau value of approximately $k_{AB}^{d}(t)/k_{AB}^{\mathrm{TST}}\approx -0.6$ for times $t>2$.

It is interesting to analyze the two-jump nonadiabatic contribution to Eq. (43) in terms of the trajectory segments appearing in the evaluation of Eq. (51). The dynamics is depicted schematically in Fig. 6.

For this contribution the trajectory starts at $t=0$ from the ground state at the top of the barrier and evolves on the ground state surface until time τ_1 where a quantum transition occurs. Between the times τ_1 and τ_2 evolution occurs on the mean surface. The jump at time τ_2 must bring the trajectory back to the ground state surface after which the evolution proceeds on the ground state until time t. Thus, one has three trajectory segments: the first and the last have no quantum phase factor but the middle trajectory segment has a nonzero

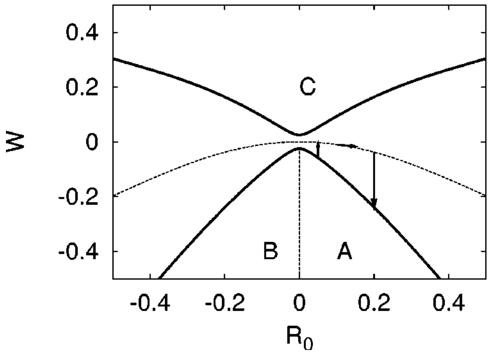

FIG. 6. Schematic representation of the sequence of the two nonadiabatic transitions giving the main contribution to the rate constant. The ground and excited state free energy surfaces are depicted by heavy lines while the light line is the mean of these two adiabatic surfaces. The temporal sequence of events proceeds from left to right. The first arrow from the ground state surface to the mean surface represents the first quantum jump. The second arrow represents the coherent propagation on the mean surface. The last arrow represents the jump from the mean surface back to the ground state with a destruction of the coherence.

phase factor arising from the coherent evolution on the mean surface $(E_1(R)+E_2(R))/2$. In Fig. 7 we show the classical time evolution of $R_0(t)$ on this mean potential energy surface.

The free-energy barrier on the mean surface is equal to 0.097 so that on this surface much more frequent, almost periodic, transitions between its left and right shallow wells are observed. This feature influences the nature of the nonadiabatic dynamics. The calculation of the contribution $k_{AB}^{d}(t)$ involves a short trajectory segment on the mean surface such that at the time τ_2 of the second jump to the ground state the coordinate $R_0(t)$ lies inside the window of $-0.25 \leqslant R_0 \leqslant 0.25$.

The calculation of $k_{AB}^{o1}(t)$ and $k_{AB}^{o2}(t)$ in Eqs. (44) and (45), respectively, depends on a knowledge of the off-diagonal part of bracket $(\hat{N}_A, \hat{\rho}_{We})_{\alpha\alpha'}$, and the off-diagonal part of the species variable $N_B^{\alpha'\alpha}(t)$, $(\alpha \neq \alpha')$. Only an odd number of nonadiabatic transitions contributes to these terms. Direct numerical evaluation of $k_{AB}^{o1}(t)$ in Eq. (44) has shown that it contributes negligibly to the rate constant.

Instead we have found that $k_{AB}^{o2}(t)$ in Eq. (45) gives a non-negligible contribution which is well approximated by events coming from a single nonadiabatic transition. The calculation of this term requires a trajectory starting at t=0 on the ground state surface and then jumping at time τ_1 onto the mean surface where it evolves until time t. In Fig. 5 we plot $k_{AB}^{o2}(t)/k_{AB}^{\mathrm{TST}}$ where one can see that for $t>2$ the contribution is close to zero but for earlier times one has a somewhat larger contribution. This term carries information about the coherent dynamics at short times but contributes negligibly to the final rate constant.

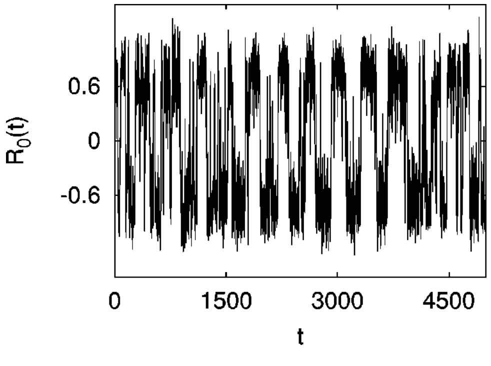

FIG. 7. Plot of the evolution of $R_0(t)$ vs time on the mean potential energy surface, $(E_1(R)+E_2(R))/2$.

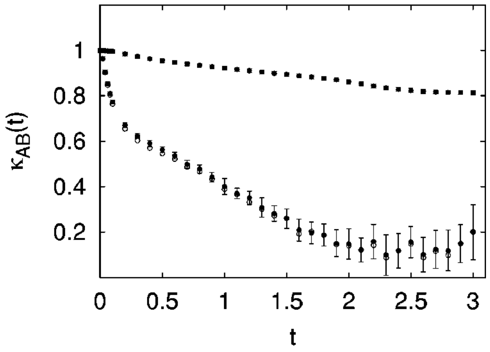

FIG. 8. Transmission coefficient $\kappa_{AB}(t)=k_{AB}(t)/k_{AB}^{\mathrm{TST}}$ vs t obtained including all nonadiabatic corrections up to two transitions (lower curve, closed circles). Also shown is $\kappa_{BA}(t)=k_{BA}(t)/k_{BA}^{\mathrm{TST}}$ (lower curve, open circles). For comparison, the upper curve shows the adiabatic transmission coefficient.

The full transmission coefficient resulting from the sum of the above-discussed adiabatic and nonadiabatic contributions is shown in Fig. 8.

The inclusion of nonadiabatic effects significantly reduces the rate constant with respect to that obtained using adiabatic dynamics. Also, the ‘‘plateau’’ is reached earlier and is seen for times $t \geqslant 2.0$.

We have also computed $k_{BA}(t)$ defined by

$$k_{BA}(t) = -(\beta \overline{n}_B^{\mathrm{eq}})^{-1} \mathrm{Tr}' \int dR\, dP\, \hat{\chi}_A(t) (\hat{\chi}_B, \hat{\rho}_{We}), \quad (60)$$

in order to check the validity of the Onsager reciprocal relations discussed in Sec. II. Since $\overline{n}_A^{\mathrm{eq}} = \overline{n}_B^{\mathrm{eq}}$ in view of the symmetry in the problem, we should have $k_{BA}(t)=k_{BA}(t)$ if the reciprocal relations were exactly satisfied. In quantum-classical dynamics the reciprocal relations are valid only to $\mathcal{O}(\mu^2)$ so that it is of interest to directly test their validity. Figure 8 also plots $\kappa_{BA}(t)$ where one sees that $\kappa_{AB}(t)$ and $\kappa_{BA}(t)$ are almost indistinguishable on the scale of the figure. Thus, the reciprocal relations are accurately satisfied indicating that the corrections are negligible for this model.

Using similar techniques we have computed $k_{AC}(t)$ defined in Eq. (35). This quantity is plotted in Fig. 9 where one sees that it starts at zero for $t=0$, reaches a maximum, and then decays to a plateau at around $t=2$ from which the rate constant $k_{AC} \approx 2 \times 10^{-5}$ can be determined. This should be compared with $k_{AB} \approx 7 \times 10^{-5}$.

VII. CONCLUSIONS

The correlation function expressions for the time-dependent rate coefficients derived in Sec. II provide the basis for the computation of these quantities using quantum-classical surface-hopping dynamics. These formulas allow one to compute the rate coefficient directly from short time

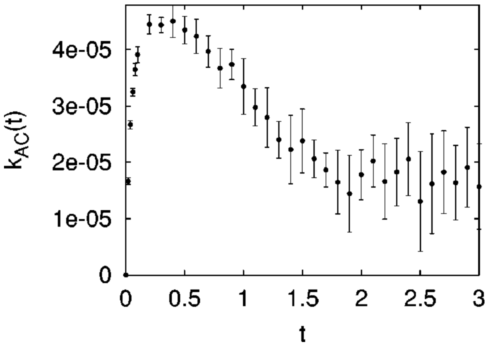

FIG. 9. The rate coefficient $k_{AC}(t)$ vs t.

nonadiabatic dynamics, rather than by simply monitoring the time evolution of a species variable over long times as is often done in mixed quantum-classical schemes. The expressions for the rate coefficient involve averages over the appropriate quantum-classical equilibrium density matrix which is stationary under the evolution, and incorporate exact surface-hopping trajectories in the framework of quantum-classical dynamics to evolve the microscopic species variables. The analysis of the Onsager coefficients corresponding to the reaction rates has established the validity of detailed balance to order μ^2 for systems obeying quantum-classical dynamics.

The explicit calculations for a two-level system coupled to a classical many-body bath have shown how the formalism may be implemented in a computational scheme. A few aspects of this calculation merit additional comment. Rather than using an exact surface-hopping algorithm[23] to compute the rate, we have employed the momentum-jump approximation[22,25] since this avoids trajectory branching and is easier to implement. This approximation leads to some difficulties discussed in the text, so it is desirable to seek simulation schemes that avoid this approximation.

The calculation algorithm we used allowed us to analyze the importance of specific nonadiabatic contributions to the rate constants. Since the trajectory segments that contribute to these nonadiabatic contributions have phase factors associated with coherent evolution segments, one gains insight into how decoherence enters the rate calculation.

The calculations have allowed us to assess the extent to which detailed balance is satisfied. For our two-state model the forward and backward rate constants are numerically indistinguishable, indicating that the predicted deviations from detailed balance in quantum-classical dynamics are negligible for this system.

Since the scheme is designed to treat arbitrary classical environments, the present results pave the way for applications of this method to more realistic systems with many classical degrees of freedom and a larger number of quantum states.

ACKNOWLEDGMENTS

This work was supported in part by a grant from the Natural Sciences and Engineering Research Council of Canada. Acknowledgment is made to the donors of The Petroleum Research Fund, administered by the ACS, for partial support of this research.

[1] T. Yamamoto, J. Chem. Phys. **33**, 281 (1960).

[2] H. B. Wang, M. Thoss, and W. H. Miller, J. Chem. Phys. **112**, 47 (2000); Y. Zhao and W. H. Miller, *ibid.* **117**, 9605 (2002); T. Yamamoto, H. B. Wang, and W. H. Miller, *ibid.* **116**, 7335 (2002).

[3] M. Topaler and N. Makri, J. Chem. Phys. **101**, 7500 (1994); J. Phys. Chem. **100**, 4430 (1996); N. Makri, J. Phys. Chem. B **103**, 2823 (1999).

[4] C. H. Mak and D. Chandler, Phys. Rev. A **44**, 2352 (1991).

[5] E. Geva, Q. Shi, and G. A. Voth, J. Chem. Phys. **115**, 9209 (2001).

[6] R. P. McRae, G. K. Schenter, B. C. Garrett, Z. Svetlicic, and D. G. Truhlar, J. Chem. Phys. **115**, 8460 (2001).

[7] C. D. Schwieters and G. Voth, J. Chem. Phys. **111**, 2869 (1999).

[8] S. Hammes-Schiffer and J. C. Tully, J. Chem. Phys. **103**, 8528 (1995).

[9] R. I. Cukier and J. J. Zhu, J. Phys. Chem. **101**, 7180 (1997); R. I. Cukier, J. Chem. Phys. **88**, 5594 (1988).

[10] S. Hammes-Schiffer and J. C. Tully, J. Chem. Phys. **101**, 4657 (1994); J. Y. Fang and S. Hammes-Schiffer, *ibid.* **110**, 11166 (1999).

[11] D. C. Borgis, S. Y. Lee, and J. T. Hynes, Chem. Phys. Lett. **162**, 19 (1989); D. C. Borgis and J. T. Hynes, J. Chem. Phys. **94**, 3619 (1991); H. Azzouz and D. C. Borgis, *ibid.* **98**, 7361 (1993).

[12] L. Xiao and D. F. Coker, J. Chem. Phys. **102**, 496 (1995); V. S. Batista and D. F. Coker, *ibid.* **110**, 6583 (1999).

[13] O. V. Prezhdo and P. J. Rossky, J. Chem. Phys. **107**, 5863 (1997).

[14] R. E. Cline, Jr. and P. G. Wolynes, J. Chem. Phys. **86**, 3836 (1987).

[15] J. C. Tully, in *Modern Methods for Multidimensional Dynamics Computations in Chemistry*, edited by D. L. Thompson (World Scientific, New York, 1998), p. 34; M. F. Herman, Annu. Rev. Phys. Chem. **45**, 83 (1994); *Classical and Quantum Dynamics in Condensed Phase Simulations*, edited by B. J. Berne, G. Ciccotti, and D. F. Coker (World Scientific, Singapore, 1998).

[16] I. V. Aleksandrov, Z. Naturforsch. A **36A**, 902 (1981).

[17] V. I. Gerasimenko, Theor. Math. Phys. **50**, 77 (1982); D. Ya. Petrina, V. I. Gerasimenko, and V. Z. Enolskii, Sov. Phys. Dokl. **35**, 925 (1990).

[18] W. Boucher and J. Traschen, Phys. Rev. D **37**, 3522 (1988).

[19] W. Y. Zhang and R. Balescu, J. Plasma Phys. **40**, 199 (1988); R. Balescu and W. Y. Zhang, *ibid.* **40**, 215 (1988).

[20] O. V. Prezhdo and V. V. Kisil, Phys. Rev. A **56**, 162 (1997).

[21] C. C. Martens and J.-Y. Fang, J. Chem. Phys. **106**, 4918 (1996); A. Donoso and C. C. Martens, J. Phys. Chem. **102**, 4291 (1998).

[22] R. Kapral and G. Ciccotti, J. Chem. Phys. **110**, 8919 (1999).

[23] S. Nielsen, R. Kapral, and G. Ciccotti, J. Chem. Phys. **112**, 6543 (2000); J. Stat. Phys. **101**, 225 (2000).

[24] S. Nielsen, R. Kapral, and G. Ciccotti, J. Chem. Phys. **115**, 5805 (2001).

[25] R. Kapral and G. Ciccotti, *A Statistical Mechanical Theory of Quantum Dynamics in Classical Environments*, in Konstanz book (Springer, Berlin, 2002), p. 455.

[26] S. R. de Groot and P. Mazur, *Non-Equilibrium Thermodynamics* (Dover, New York, 1984).

[27] N. Makri and K. Thompson, Chem. Phys. Lett. **291**, 101 (1998); K. Thompson and N. Makri, J. Chem. Phys. **110**, 1343 (1999); N. Makri, J. Phys. Chem. B **103**, 2823 (1999).

[28] D. MacKernan, R. Kapral, and G. Ciccotti, J. Chem. Phys. **116**, 2346 (2002).

[29] M. Tuckerman, B. J. Berne, and G. J. Martyna, J. Chem. Phys. **97**, 1990 (1992).

[30] D. Chandler, J. Chem. Phys. **68**, 2959 (1978).

[31] D. MacKernan, R. Kapral, and G. Ciccotti, J. Phys.: Condens. Matter **14**, 9069 (2002).

[32] C. Wan and J. Schofield, J. Chem. Phys. **112**, 4447 (2000).

[33] I. Horenko, C. Saltzmann, B. Schmidt, and C. Schutte, J. Chem. Phys. **117**, 11075 (2002).